The effects of impurity scattering and transport topology on trapping in quasi-one-dimensional systems: Application to excitons in molecular crystals

R. D. Wieting, M. D. Fayer,[a] and D. D. Dlott

Department of Chemistry, Stanford University, Stanford, California 94305
(Received 6 March 1978)

A model is developed which permits a detailed examination of the effects of impurity scattering and deviations from a strictly one-dimensional transport topology on the trapping rate and on the mean-square displacement of mobile species in systems which are nearly one-dimensional in their transport characteristics, i.e., quasi-one-dimensional. The model is applied specifically to Frenkel excitons in molecular crystals, but may be readily adapted to other types of systems. Both coherent (wavelike) and incoherent (diffusive) microscopic modes of exciton transport are considered. In the strictly one-dimensional limit following pulsed optical excitation, a time-dependent trapping rate function is obtained as opposed to the commonly employed trapping rate constant. It is demonstrated that the coherent and incoherent trapping rate functions have identical dependencies on time and on impurity concentration and the macroscopic rate of transport can be calculated. To treat deviations from strictly one-dimensional transport topology, it is necessary to consider anisotropic walks on the system's "superlattice," i.e., the array of molecular chain segments which are bounded by scattering impurities. Montroll's Green function formalism is employed to obtain solutions to various walk topologies which have not previously been reported in the literature. In the quasi-one-dimensional case, a time-dependent trapping rate function is also obtained unless the walk on the superlattice is nearly isotropic. The various trapping rate functions are then employed to provide explicit expressions for the time-dependent trap population which is proportional to the intensity of time resolved optical emission, a widely used experimental observable. Finally, the exciton mean-square displacement for a quasi-one-dimensional system with scattering impurities is shown to remain basically one dimensional even in situations where exciton trapping behaves in a manner best described in terms of a three-dimensional topology.

I. INTRODUCTION

Systems which exhibit near-one-dimensional energy transport are currently a topic of extensive experimental and theoretical research. These include exciton and electron transport in biopolymers, electron transport in organic polymers (SN_x), electron transport in organic metals (TCNQ-type salts), and electron and exciton transport in organic molecular crystals.[1] In the following we will develop a model for Frenkel exciton dynamics in one-dimensional organic molecular crystals which may also be adapted to these other systems. Previously, most attention has been focused on phonon interactions and on the magnitude of the intermolecular interaction responsible for the one-dimensional exciton transport.[2] In order to develop a model for exciton dynamics which closely resembles the situation found in actual experimental samples, it is also necessary to consider the effects of impurities and deviations from a strictly one-dimensional transport topology. Systems which are close to, but not strictly one-dimensional, will be referred to as quasi-one-dimensional systems. Impurities, which may be isotopic, chemical, or lattice defects, can be of two types. Those which have an excited state energy level below that of the corresponding host crystal exciton band can inhibit exciton transport by localizing, i.e., trapping, a mobile exciton.[3] Impurities with energy levels above that of the corresponding host crystal exciton band can scatter a mobile exciton, also inhibiting transport.[4] In either case, a well-defined impurity site will exist if S, the difference in energy between the impurity level and the band center, is large relative to β, the intermolecular interaction matrix element responsible for exciton transport, i.e., $S \gg \beta$.[5] (If $S \approx \beta$, the impurity level will be amalgamated into the band and will produce nonlocal scattering.[6])

Previously, it has been demonstrated that impurity scattering sites in low concentration can dramatically alter the nature of transport in one-dimensional crystals, causing microscopically wavelike transport (coherent), to be macroscopically diffusive.[4] In another study, the effect of scattering sites on exciton transport which is microscopically incoherent, i.e., microscopically diffusive, was discussed.[7] In both cases, caging the exciton between scattering impurities transforms rapid exciton motion along the principal axis into a smaller net macroscopic displacement involving a comparatively slow stepping frequency between adjacent cages. Since $S \gg \beta$, the transmission probability past the impurity is small and excitons remain caged long enough for the time-averaged probability to become uniform.[4] Migration can be thought of as a random walk between linear cages, "supersites," on a lattice of cages, a "superlattice."

In addition to reducing the exciton mean-square displacement along the one-dimensional axis, caging of the exciton can have other important consequences which were not considered in previous studies. In a real system, almost negligible interchain interactions give rise to infrequent steps to parallel one-dimensional chains of molecules. Since scattering impurities obstruct migration only along the principal axis, the along-chain

[a] Alfred P. Sloan Fellow.

 0021-9606/78/6905-1996$01.00

cage stepping frequency can be comparable to the cross-chain frequency. Thus, while such a crystal has an exciton band dispersion which is one-dimensional, its exciton transport may behave as a random walk on a two- or three-dimensional superlattice. This changes the character of the exciton transport since multidimensional walks greatly increase the total number of distinct lattice sites sampled[8] and consequently increase the ability of an exciton to reach a distant trap site.

Time-resolved optical emission from trap states has frequently been used as a probe of both singlet and triplet exciton dynamics.[4,9] The main focus of this work is to describe the influence of impurity scattering and small multidimensional interactions on the time dependence of exciton trapping and on the exciton mean-square displacement in quasi-one-dimensional systems. To this end, the strictly one-dimensional problem is treated. A more restricted solution for the coherent one-dimensional problem has previously been applied to the trapping of triplet excitons in 1, 2, 4, 5-tetrachlorobenzene (TCB) crystals at low temperature. In the TCB system, which is basically one-dimensional, the naturally occurring isotopic impurity monodeutero-TCB (0.03% abundance) produces well-defined scattering sites. The preliminary theory was able to come close to reproducing the experimental trapping data without adjustable parameters, demonstrating the need to consider the effect of impurity scattering on trapping in one-dimensional systems. Here we present general solutions to the incoherent and coherent problem, and the quasi-one-dimensional problem.

Caging an exciton greatly extends the exciton–trap interaction time in cages which have trap sites and consequently those cages act as "supertraps." Thus, entering such a cage always results in trapping[4] even if the single encounter trapping probability is quite small, and irrespective of the detailed description[10] of the trapping event. The two limiting cases of exciton–phonon scattering are treated. Either exciton–impurity scattering greatly dominates exciton–phonon scattering (microscopically coherent) or exciton–phonon scattering greatly dominates exciton–impurity scattering (microscopically incoherent). The case in which the rates of exciton–phonon scattering and exciton–impurity scattering are comparable could be treated using, for example, the Knox and Kenkre[11] or Silbey[12] formalisms to recalculate the cage escape time [Eqs. (6) and (10)]. The rest of the development of the sampling functions and trapping rate functions presented below would remain unchanged.

Recently, several experimental studies[9(b)] of trapping in quasi-one-dimensional exciton systems have employed a phenomenological *trapping rate constant* to analyze the trapping experiments and to infer the microscopic details of exciton transport. It will be demonstrated below that in the strictly one-dimensional case, a time-dependent trapping rate function is obtained—not a rate constant. The trapping rate constant is a rigorous result only in the long time limit of virtually isotropic transport on the superlattice. Since dilute traps in one dimension are separated by large distances, the trapping rate function can be used to determine the macroscopic rate of transport which is in turn determined by the details of microscopic transport.

A physical parameter which is readily varied in an experimental sample is the concentration of scattering impurities. A good deal of experimental work has been performed using this approach in disordered solids in which the effect of large concentrations (~50%) of impurities is considered.[13] For low impurity concentration quasi-one-dimensional systems, two new results emerge. First, the dependence of the trapping rate on scattering impurity concentration is the same for both the coherent and incoherent modes of transport, and therefore it is not possible to infer the microscopic mode of transport from a concentration study alone. Second, the rate of trapping varies only gradually with the scattering impurity concentration although this is contrary to some common intuitive ideas. These results will be used subsequently to interpret data obtained from a concentration study of time resolved trap emission in TCB at low temperature.[14]

II. THE TRAPPING RATE EQUATIONS

The model presented here considers a single exciton population ensemble, e.g., a singlet exciton band or, in the absence of spin–lattice relaxation, one triplet spin sublevel exciton band, interacting with dilute impurities. N_T is the mole fraction of trapping impurities and χ is the mole fraction of scattering impurities. The case of interest is where $1 \gg \chi > N_T$. As discussed above, in quasi-one-dimensional systems with scattering sites, all traps behave as supertraps, and therefore the trapping rate function is directly related to $S(t)$, the number of distinct lattice sites sampled by the exciton from time $t=0$ to time t. The instantaneous rate of exciton localization per unit population, the trapping rate function, is given by (see Appendix A)

$$K_L(t) = \ln\left(\frac{1}{1-N_T}\right)\frac{dS(t)}{dt}\ , \tag{1a}$$

and since $\ln(1/1-N_T) = N_T$ for small N_T,

$$K_L(t) = N_T\frac{dS(t)}{dt}\ . \tag{1b}$$

Equation (1b) has been employed previously with its derivation based on physical arguments.[15] The form of $S(t)$, and thus of $K_L(t)$, is dependent on the mode and dimensionality of the transport. As noted in a recent review of singlet exciton energy transfer,[9(a)] $K_L(t)$ may be considered to be the fundamental observable in trapping experiments. If $\dot{S}(t)$ is time independent, then $K_L(t)$ becomes a trapping rate constant. However, in general, $K_L(t)$ is a time-dependent trapping rate function.

For an ensemble of excitons, the time-dependent populations of the band states $E(t)$ and trap states $T(t)$ are described, respectively, by the rate equations

$$\dot{E}(t) = -[K_E + K_L(t)]E(t)\ , \tag{2a}$$

$$\dot{T}(t) = -K_T T(t) + K_L(t)\,E(t). \tag{2b}$$

K_E is the decay rate constant for band states in the ab-

sence of trapping and K_T is the decay rate constant for trap states. At sufficiently low temperatures, thermally assisted promotion from a localized state to a mobile band state is negligible[16] and therefore will not be considered.

Equations (2a) and (2b) are solved for initial conditions $E(0)=1$ and $T(0)=0$. This corresponds to impulse optical excitation of the sample in a manner producing partially or totally localized excitons which are on the average far removed from the dilute traps. This initial condition will occur, for example, if excitation takes place into a high lying vibration of the excited state. The poor Franck–Condon factors will cause the intermolecular interactions to be small relative to the local potential fluctuation and therefore the exciton is self-trapped. Radiationless relaxation to the vibrationally unexcited exciton band will be basically an intramolecular process. Once in this band, the Franck–Condon overlap increases and exciton transport can be coherent or incoherent. Under the special condition that narrow band excitation of the exciton origin ($k=0$) is used, a highly delocalized initial state can result and $E(0)$ and $T(0)$ may have to be chosen differently. Inserting Eq. (1) into Eq. (2) gives

$$E(t)=\exp[-K_E t - N_T S(t)], \tag{3a}$$

$$T(t)=\exp(-K_T t)\int_0^t N_T \dot{S}(t') \times \exp[-(K_E-K_T)\,t' - N_T S(t')]\,dt' . \tag{3b}$$

These equations provide a route, from the observed time resolved emission through $S(t)$, to the factors influencing exciton transport.

III. EXCITON TRAPPING AND THE SAMPLING FUNCTION $S(t)$

At time $=t$, the number of distinct lattice sites visited by an exciton is $S(t)$. Exciton transport is a random walk on the superlattice with the cage stepping frequency determined by the microscopic mode of transport. The sampling function gives the total number of distinct *sites* sampled, which is the product of cage size and number of supersites sampled:

$$S_{\mathrm{SITES}}(t)=(\text{cage size})\times S_{\mathrm{CAGES}}(t). \tag{4}$$

E. W. Montroll developed a Green's function formalism for calculating the properties of random walks on lattices of various dimensionality and configuration.[8,17] Montroll's approach is used to determine $S(t)$ for a variety of transport topologies and the population equations [Eq. (3)] are solved.

A. Cage stepping frequency for strictly one-dimensional transport

When exciton–impurity scattering dominates exciton–phonon scattering, exciton transport is microscopically coherent. In a lattice containing periodically substituted scattering sites, the stepping frequency for a particular k state is given by Eq. (3) of Ref. 4

$$\nu_I(k)=\left|\frac{16\pi\beta^3}{hS^2 l}\sin^3 ka\right| , \tag{5}$$

where a is the lattice spacing and $la=(\chi^{-1}-1)\,a$ is the cage size. If the exciton band is in thermal equilibrium at temperature T, an ensemble average over k states yields the thermal average stepping frequency of coherent excitons between cages[18]

$$\nu_{\mathrm{COH}}(T)=\frac{16\pi^{1/2}}{\chi^{-1}-1}\,\frac{|\beta|^3}{hS^2}\,\frac{I_{3/2}(y)}{(y/2)^{3/2}I_0(y)} , \tag{6}$$

where $y=|2\beta/KT|$ and I_0 and $I_{3/2}$ are modified Bessel functions. This result will also be useful in Sec. III. C when small interactions between parallel one-dimensional chains are considered. Real crystals contain a random distribution of scattering impurities, and this result is obtained in Sec. III. B.

When exciton–phonon scattering is fast relative to the time required for an exciton to move one lattice site in a wavelike manner, the k state dependent details of migration are averaged out and exciton motion is a microscopic random walk from site to site. The microscopic stepping frequency ν_{INC} can be calculated using the formalism of Kenkre and Knox[19] and is given by

$$\nu_{\mathrm{INC}}=\frac{16\pi^2\beta^2}{\alpha h^2} . \tag{7}$$

This result assumes that the memory function for loss of coherence decays exponentially with rate α. α can be obtained from spectroscopic information if the absorption line shape is Lorentzian.

The effect of scattering impurities on incoherent exciton transport was considered for a periodic distribution of scattering sites.[7] In that treatment the exciton probability must first achieve near uniform density in the cage and then a random step can be made to either adjacent cage. If the cage is too large, uniform density is not achieved and the procedure is not applicable. This sets a minimum concentration of impurities for which a calculation can be performed. The stepping frequency between adjacent cages is given by

$$\nu_{\mathrm{INCOH}}=\frac{T\nu_{\mathrm{INC}}}{l}\left(\frac{1-P_e}{2P_e}\right)\ln\left(\frac{1+P_e}{1-P_e}\right) , \tag{8a}$$

$$P_e=1-(1-T)^{\langle n\rangle+1} , \tag{8b}$$

$$\langle n\rangle=l\left(\frac{2}{\pi}\right)^{1/2}\left(1+\frac{3}{8l^2}-\frac{7}{128l^4}+\cdots\right) . \tag{8c}$$

P_e is the probability of escape from the initial cage before a uniform distribution is achieved and $\langle n\rangle$ is the mean number of exciton collisions with the nearest impurity site before a uniform distribution is achieved. T is the transmission probability for a single exciton–impurity collision, ν_{INC} is the microscopic exciton stepping frequency, and the cage size la is the average size for a mole fraction χ of scattering impurities. A reasonable estimate of T can be obtained by taking the exciton to be a Wannier function, i.e., composed of equal weights of all k states. Using the penetration probability for a single k state[4] and averaging yields

TABLE I. The cage stepping frequency ν_{COH} between adjacent cages along a one-dimensional chain of molecules for an ensemble of coherent excitons at 1.4 °K [Eq. (6)]. The bandwidth is $4\beta = 40\ cm^{-1}$.

	ν_{COH} (sec^{-1}) Impurity concentration		
s/β	10^{-1}	10^{-2}	10^{-3}
10	2.7×10^{8}	2.5×10^{7}	2.4×10^{6}
33	2.5×10^{7}	2.3×10^{6}	2.2×10^{5}
100	2.7×10^{6}	2.5×10^{5}	2.4×10^{4}

$$T = \langle \phi(k) \rangle = \frac{2\beta^2}{S^2} \quad . \tag{9}$$

Substituting, the stepping frequency of incoherent excitons between supersites is

$$\nu_{INCOH} = \frac{\nu_{INC}}{\chi^{-1}-1}\ \frac{\beta^2}{S^2}\left(\frac{1-P_e}{P_e}\right)\ln\left(\frac{1+P_e}{1-P_e}\right), \tag{10a}$$

and, if Eq. (7) is applicable,

$$\nu_{INCOH} = \frac{16\pi^2\beta^4}{(\chi^{-1}-1)\alpha h^2 S^2}\left(\frac{1-P_e}{P_e}\right)\ln\left(\frac{1+P_e}{1-P_e}\right). \tag{10b}$$

This result is also used when small interactions between adjacent chains are considered.

Equations (6) and (10) give the stepping frequency between supersites for coherent and incoherent excitons. As the concentration of scattering impurities increases, the stepping frequency increases since there are more frequent encounters at the ends of the cage. However, the distance per step decreases and the net effect is to reduce the transport rate. The transmission probability is inversely proportional to S/β, where S is the energy gap between the center of the band and the impurity and β is the intermolecular interaction. For coherent excitons the transport rate also depends on β/KT, where T is the temperature, since the coherent group velocity is sensitive to thermal partitioning of excitons among the k states.[4,18] Table I presents the stepping frequency for coherent excitons having a bandwidth of 40 cm^{-1}. This would correspond to a large triplet band or a small singlet band. Table II presents the results for incoherent excitons, where the microscopic hopping frequency ν_{INC} has been set equal to 10^{12} sec^{-1}. These tables illustrate the effect of cage size and band impurity separation on the stepping frequency.

B. Strictly one-dimensional sampling and trapping rate equations

In this section, the sampling function and trapping rate function for a strictly one-dimensional lattice are calculated. It is a well-known result that random walks in one dimension sample distinct sites of the lattice (in this case supersites on the superlattice) according to[8]

$$S(t) = \left(\frac{8\nu t}{\pi}\right)^{1/2}\{1 + o\,[(\nu t)^{-1}]\}, \tag{11}$$

where ν is the stepping frequency and $o(x)$ signifies "terms on the order of x." In nearly all cases, these terms decay very quickly and are neglected.

For coherent excitons migrating amongst randomly distributed impurities (hence between randomly sized cages), the sampling function [Eq. (4)], for each k state and each cage length l is

$$S^k(t) = l\left[\frac{8\nu_l(k)t}{\pi}\right]^{1/2}, \tag{12}$$

where $\nu_l(k)$ is given by Eq. (5). Averaging over the impurity distribution function $P(l) = \chi(1-\chi)^l$ yields

$$\overline{S^k(t)} = \left|\frac{2^{5/2}\pi^{1/2}\chi}{[\ln(1/1-\chi)]^{3/2}}\ \frac{\beta^{3/2}}{h^{1/2}S}\sin^{3/2}ka\right| t^{1/2}. \tag{13}$$

If the exciton–phonon scattering rate is fast enough to maintain thermal equilibrium and slow relative to the exciton–impurity scattering rate, an ensemble average[4,18] over k states gives the thermal average site sampling function

$$S(t) = \left\{\frac{2^{5/2}\Gamma(5/4)\chi}{[\ln(1/1-\chi)]^{3/2}}\ \frac{I_{3/4}(y)}{(y/2)^{3/4}I_0(y)}\ \frac{|\beta|^{3/2}}{h^{1/2}S}\right\} t^{1/2}, \tag{14}$$

where $y = |2\beta/KT|$ and I_0 and $I_{3/4}$ again are modified Bessel functions.

Substitution of $S(t)$ into Eq. (1) gives the trapping rate function for microscopically coherent transport in one dimension,

$$K_L(t) = A_{COH}\, t^{-1/2}, \tag{15}$$

where the time-independent parameter A_{COH} is given by

$$A_{COH} = \frac{2^{3/2}\Gamma(5/4)I_{3/4}(y)}{(y/2)^{3/4}I_0(y)}\ \frac{N_T\chi}{[\ln(1/1-\chi)]^{3/2}}\ \frac{|\beta|^{3/2}}{h^{1/2}S}. \tag{16}$$

It should be noted that Eqs. (15) and (16) are more general than the Gaussian diffusion model of exciton migration and trapping used in Ref. 4. An important feature of Eq. (16) is that all the necessary parameters β, S,

TABLE II. The cage stepping frequency ν_{INCOH} between adjacent cages along a one-dimensional chain of molecules for an ensemble of incoherent excitons [Eq. (10). The microscopic hopping frequency has been set to $\nu_{INC} = 10^{12}$ sec^{-1}, and $\nu_{INCOH} \propto \nu_{INC}$.

	ν_{INCOH} (sec^{-1}) Impurity concentration		
s/β	10^{-1}	10^{-2}	10^{-3}
10	1.9×10^{9}	5.5×10^{7}[a]	b
33	2.0×10^{8}	1.6×10^{7}	5.6×10^{5}[a]
100	2.2×10^{7}	2.0×10^{6}	1.7×10^{5}

[a]These results are approximate. See discussion surrounding Eq. (8).
[b]Equation (8) is inapplicable.

χ, and T can be independently experimentally determined. The observed time resolved trap emission is proportional to the trap population and therefore can be calculated for an exciton system which is microscopically coherent and strictly one-dimensional.

The number of distinct lattice sites sampled by an incoherent exciton is found by combining Eqs. (4) and (11):

$$S(t) = \frac{|\beta|}{S}\left[\frac{8(\chi^{-1}-1)\nu_{\mathrm{INC}}}{\pi}\left(\frac{1-P_e}{P_e}\right)\times\ln\left(\frac{1+P_e}{1-P_e}\right)\right]^{1/2} t^{1/2} . \quad (17)$$

Using Eq. (1), we obtain the trapping rate function for incoherent excitons in one dimension

$$K_L(t) = A_{\mathrm{INCOH}}\, t^{-1/2} \quad (18)$$

and

$$A_{\mathrm{INCOH}} = \frac{N_T|\beta|}{S}\left[\frac{2(\chi^{-1}-1)\nu_{\mathrm{INC}}}{\pi}\left(\frac{1-P_e}{P_e}\right)\times\ln\left(\frac{1+P_e}{1-P_e}\right)\right]^{1/2} \quad (19a)$$

$$= \frac{4\pi\beta^2 N_T}{hS}\left[\frac{2(\chi^{-1}-1)}{\alpha\pi}\left(\frac{1-P_e}{P_e}\right)\times\ln\left(\frac{1+P_e}{1-P_e}\right)\right]^{1/2} , \quad (19b)$$

where Eq. (19b) has used Eq. (7) for ν_{INC}. Both microscopic modes of transport yield the same functional dependence on time. This is because both modes of migration result in a random walk among the supersites on a time scale long relative to the impurity scattering time. For coherent excitons, the trapping rate coefficient $A_{\mathrm{COH}} \propto \chi/[\ln(1/1-\chi)]^{3/2}$. However, for relatively dilute impurities, $\ln[1/1-\chi]=\chi$, so that the trapping rate coefficient $A_{\mathrm{COH}} \propto \chi^{-1/2}$, which is the same dependence manifested by A_{INCOH} [Eq. (19)] for incoherent excitons. The $\chi^{-1/2}$ dependence on concentration is thus a strict test for one-dimensional transport regardless of the microscopic mode of migration.

The effect of various concentrations of impurities on the trapping rate coefficient is shown in Table III for coherent excitons at 1.4 °K with a bandwidth of 40 cm^{-1}, and in Table IV for incoherent excitons where the microscopic hopping time has been chosen to be $\nu_{\mathrm{INC}}^{-1}=1$ psec. Tables III and IV give the coefficients of $t^{-1/2}$ in the trapping rate function $K_L(t)$, where from Eqs. (15) and (18), $K_L(t)=At^{-1/2}$. Various values of band–impurity energy separation S are used. Increasing S decreases the trapping coefficient. As the impurity concentration becomes larger, the step length becomes smaller faster than the step frequency increases, thus decreasing the trapping coefficient.

TABLE III. The trapping rate coefficient A_{COH} for coherent excitons at 1.4 °K on a strictly one-dimensional chain of molecules containing dilute scattering impurities and traps [Eq. (16)]. The concentration of traps is 5×10^{-5}. The bandwidth $4\beta = 40$ cm^{-1}.

	A_{COH} ($\mathrm{sec}^{-1/2}$)		
	Impurity concentration		
S/β	10^{-1}	10^{-2}	10^{-3}
10	3.5	12	38
33	1.1	3.6	12
100	0.35	1.2	3.8

TABLE IV. The trapping rate coefficient A_{INCOH} for incoherent excitons on a strictly one-dimensional chain of molecules containing dilute scattering impurities and traps [Eq. (16)]. The concentration of traps is 5×10^{-5}. The incoherent hopping frequency is 10^{12} sec^{-1}, and $A_{\mathrm{INCOH}} \propto \nu_{\mathrm{INC}}^{1/2}$.

	A_{INCOH} ($\mathrm{sec}^{-1/2}$)		
	Impurity concentration		
S/β	10^{-1}	10^{-2}	10^{-3}
10	16	29[a]	b
33	5.1	16	30[a]
100	1.7	5.6	16

[a]These results are approximate. See the discussion surrounding Eq. (8).
[b]Equation (8) is inapplicable.

The population rate equations can now be solved. Since both modes of transport have the same form of the trapping rate function, $K_L(t)=At^{-1/2}$, inserting this form into Eq. (3) yields

$$E(t) = \exp(-K_E t - 2At^{1/2}) , \quad (20a)$$

$$T(t) = \exp(-K_T t)\left(\frac{\pi A^2}{K_E-K_T}\right)^{1/2}\exp\left(\frac{A^2}{K_E-K_T}\right)\left(\mathrm{erf}\left\{[(K_E-K_T)t]^{1/2}+\frac{A}{(K_E-K_T)^{1/2}}\right\}-\mathrm{erf}\left[\frac{A}{(K_E-K_T)^{1/2}}\right]\right) ,$$

where $\mathrm{erf}(x)$ is the error function of argument x. If $K_E=K_T=K$, then these solutions are

$$E(t) = \exp(-Kt - 2At^{1/2}) , \quad (21a)$$

$$T(t) = \exp(-Kt)[1-\exp(-2At^{1/2})] , \quad (21b)$$

where A is given by Eq. (16) or (19) for coherent or incoherent excitons, respectively.

The time-dependent trap population is displayed in Fig. 1. To illustrate triplet systems, a lifetime of 20 msec for the exciton band and of 50 msec for the trap state is used. A range of trapping coefficients is displayed. These values of A could result from a variety of conditions, e.g., mode of transport, β, S, coherence decay rate α, scattering impurity concentration, and temperature. Note that larger values of A cause a very abrupt rise in the trap population, while smaller values

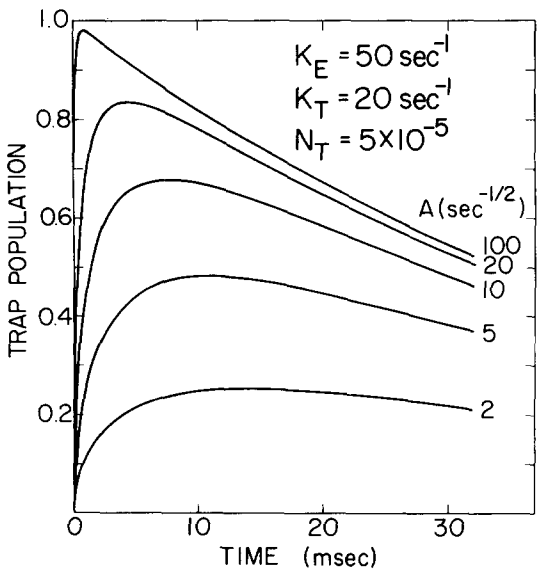

FIG. 1. Calculated trap populations as a function of time are used to illustrate the effect of increasing the coefficient A of the time-dependent trapping rate function for strictly one-dimensional transport on the time-dependent intensity of trap emission following impulse optical excitation of the exciton band. Each curve can be arrived at from a variety of possible combinations of the parameters which affect the nature of exciton transport. The rate constants for the exciton and trap decay, K_E and K_T respectively, are 50 and 20 sec^{-1}. These rates are typical of triplet systems. As A is increased, the population maximum is shifted to shorter times and the integrated population of the trap increases.

shift the maximum to longer times. As A decreases, the total integrated trap population decreases and more emission would be observed from the exciton band.

C. Quasi-one-dimensional sampling and trapping rate equations

A complete model of a one-dimensional system must allow for nonvanishing interactions between adjacent chains of the ensemble. An exciton is localized in a cage by the impurities and confined on a chain by small cross-chain interactions, but in the general case can still execute a random walk on a three-dimensional superlattice whose supersites are the linear cages of molecular lattice sites. For the calculations presented below, two different three-dimensional arrangements of chains will be used to provide lower and upper bounds to the three-dimensional trapping function $K_L(t)$. In both cases, the discussion of Sec. II concerning trapping sites applies, i.e., any supersite containing a trap site within it will behave as a supertrap.

In the calculations presented below, the results for the two different topologies will be obtained by employing the procedure developed by E. W. Montroll.[8,17] For each topology, there is a set of neighboring supersites to which a step can be made, and a corresponding set of step probabilities. The Fourier expansion of the stepping probability function is called the structure function $\lambda(\phi)$ of the random walk. This is easily constructed from a set of the vector displacements and corresponding probabilities. The appropriate function $\lambda(\phi)$ is then inserted into the expression for the generating function of all walks which end at the origin, the Green's function $U(z, 0)$. Employing a Tauberian theorem, the number of distinct lattice sites sampled in a walk of n steps $S(n)$ is then obtained from the asymptotic behavior of $U(z, 0)$ as $z \to 1$.

The lower limit properties are obtained from an arrangement of the one-dimensional chains in which all of the chains and all of the scattering sites are aligned in the horizontal and the vertical direction (see Fig. 2). This provides a lower bound for the sampling of distinct lattice sites because a scattering site cannot be bypassed via off-chain exciton motion. This minimizes the sampling of distinct sites. The lattice arrangement forms a simple cubic topology and steps occur to cage positions $(\pm 1, 0, 0)$ along the one-dimensional direction or to cage positions $(0, \pm 1, 0)$ or $(0, 0, \pm 1)$ on adjacent chains. The random walk structure function $\lambda(\phi_1, \phi_2, \phi_3)$ for this topology has been given as[8]

$$\lambda_{\mathfrak{L}}(\phi_1, \phi_2, \phi_3) = L\cos\phi_1 + C\cos\phi_2 + C'\cos\phi_3, \qquad (22)$$

where ϕ_i is the displacement variable on the ith axis. The constants L, C, and C' are the probabilities of steps to cage locations $(\pm 1, 0, 0)$, $(0, \pm 1, 0)$, and $(0, 0, \pm 1)$, respectively.

The upper limit properties are obtained from an arrangement comprised of staggered layers of planes, each plane consisting of staggered cages, as shown in Fig. 3. This arrangement maximizes the ability of an exciton to bypass the scattering impurities by motion

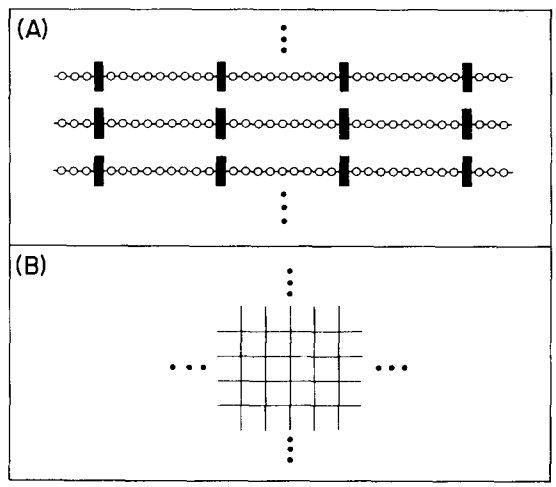

FIG. 2. (A) A cross section of the infinite three-dimensional lattice consisting of one-dimensional chains of molecular lattice sites (open circles) containing periodic substitutional scattering impurities (solid bars). The chains are arranged so that all the imputities lie in parallel planes. An exciton may step from a given cage to either neighbor along the chain, or to one of four neighbors in orthogonal directions. This arrangement provides a lower bound for the rate of sampling of new cages since excitons must tunnel through an impurity to move in the one-dimensional direction. The topology is that of a simple cubic lattice. (B) The same lattice is viewed in cross section from the one-dimensional direction, where each linear chain is represented by a square.

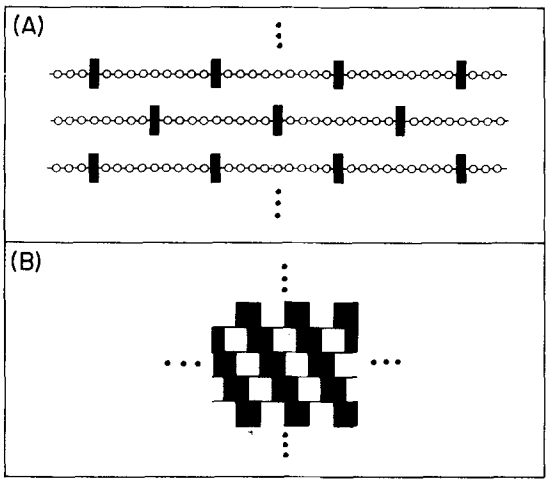

FIG. 3. (A) A cross section of the upper bound lattice consisting of one-dimensional chains of molecular lattice sites (open circles) containing periodic substitutional scattering impurities (solid bars). In a single plane, alternate chains are arranged so that each scattering impurity site lies next to the centers of the cages on the neighboring chains. In this staggered topology no two neighboring linear cages are completely aligned with each other. This provides an upper bound for the rate of sampling of new cages, since steps in directions orthogonal to the chains can allow transport along the chains without tunneling past a scattering site. For further discussion see Appendix B. (B) The same lattice is viewed from the one-dimensional direction in a cross section containing impurity sites. The dark squares indicate impurity sites in a plane of the cross section and the light squares impurity sites one-half cage length from the plane of the cross section. Each successive layer of chains is shifted one half the chain separation.

off of a chain, thus maximizing the sampling of distinct lattice sites. The random walk structure function for this staggered topology is developed in Appendix B, where a more detailed discussion of this lattice is included. The result is

$$\lambda_U(\phi_1,\ \phi_2,\ \phi_3) = L\cos\phi_1 + C\cos\phi_1\cos\frac{\phi_2}{2} + \frac{1}{2}C'\left[\cos\left(\frac{\phi_2}{2}-\phi_3\right)+\cos\frac{\phi_1}{2}\cos\left(\frac{\phi_2}{2}+\phi_3\right)\right] \quad (23)$$

where the ϕ_i are the same as before and the constants L, C, and C' represent the relative probabilities of a step to one of three distinct sets of cage locations. These probabilities for both topologies are given by

$$\begin{aligned} &\text{On chain} \quad 1D \text{ direction:} \quad L = \nu_L/\nu_{\mathrm{TOT}}\ , \\ &\text{Interchain} \begin{cases} \text{in plane:} & C = \nu_C/\nu_{\mathrm{TOT}} \\ \text{out of plane:} & C' = \nu_{C'}/\nu_{\mathrm{TOT}}\ , \end{cases} \quad (24) \\ &\nu_{\mathrm{TOT}} = \nu_L + \nu_C + \nu_{C'}\ . \end{aligned}$$

The frequency of steps in the one-dimensional direction ν_L is taken from Sec. III. A, Eq. (6) or Eq. (10), depending on the microscopic mode of transport. The structure function and thus the trapping rate function can be calculated for arbitrary values of the small off-chain stepping frequencies ν_C and $\nu_{C'}$.

The site sampling function is obtained for these three-dimensional structure functions through the Green's function of all walks which end at the origin,

$$U(z,\ 0) = \frac{1}{(2\pi)^3}\iiint_{-\pi}^{\pi}\frac{d\phi_1 d\phi_2 d\phi_3}{1 - z\lambda(\phi_1,\ \phi_2,\ \phi_3)}\ . \quad (25)$$

The number of distinct lattice positions sampled by a walker after n steps $S(n)$ can be obtained through the expansion of $U(z,\ 0)$ as $z \to 1$, followed by the application of a Tauberian theorem to the expansion.[8] Thus

$$S(n) = \frac{\mathcal{C}(n)}{u_0}\, n\ , \quad (26a)$$

where

$$\mathcal{C}(n) = 1 + \frac{2u_1}{\pi^{1/2}u_0}\, n^{-1/2} + \mathcal{O}(n^{-1})\ . \quad (26b)$$

The number of new sites per step is thus a constant, given by u_0^{-1}, in the asymptotic limit of large n, since the corrections to unity in Eq. (26b) will vanish and $\mathcal{C}(n) \to 1$. For nearly all cases, the terms $\mathcal{O}(n^{-1})$ decay very rapidly compared to the first two terms of Eq. (26b) and can be neglected. The functional form of $S(n)$ [Eq. (26a)] will become a sum of two terms, one proportional to n and the second proportional to $n^{1/2}$. The constants u_0 and u_1 are given by

$$u_0 = U(1,\ 0), \quad (27)$$

$$u_{1\mathcal{L}} = 1/(2\pi^2 LCC')^{1/2}\ , \quad (28a)$$

$$u_{1\mathcal{U}} = 1/\left[2\pi^2\left(L + \frac{C}{4} + \frac{C'}{8}\right)\left(C + \frac{C'}{4}\right)C'\right]^{1/2}\ , \quad (28b)$$

where $u_{1\mathcal{L}}$ and $u_{1\mathcal{U}}$ (see Appendix B) are the expressions obtained from lower and upper bound walk topologies, respectively. u_0 must be evaluated using Eq. (25) with $z = 1$ and the structure function $\lambda(\phi)$ appropriate to the walk topology. The triple integral $U(1,\ 0)$ is convergent for any three-dimensional topology[8] and may be obtained by numerical integration.

The behavior of the sampling function [Eq. (26)] for lower and upper bounds is illustrated by Tables V and VI. Anisotropy in the random walk tends to increase the importance of the correction term in Eq. (26b), particularly when relatively few steps have been made. Thus, Eq. (26) is not the best form of the sampling function when the walk is approaching the one- or two-dimensional limit. In those limits the analysis must back up to the random walk structure function appropriate to the dimensionality, e.g., with $C = C' = 0$ or $C' = 0$, and derive the form of $S(n)$ from the $z \to 1$ divergent behavior of the Green's function [Eq. (25)]. The one-dimensional problem is treated in Section B and the two-dimensional problem in Appendix C. In nearly isotropic situations the sampling function is linear in time. This is true for the upper and lower bound topologies, although a comparison of the tables shows that the importance of the correction term decreases for the staggered topology compared to the cubic topology. The staggered topology emphasizes the three-dimensional character of the walk, as well as increases the absolute rate of sampling. Note that the lower and upper bound topologies give virtually the

TABLE V. Three-dimensional random walk sampling parameters for the lower bound (simple cubic) topology (Fig. 2). The interchain step probabilities [Eq. (24)] C and C' have been set equal. $L+C+C'=1$.

Along-chain step probability L	u_0^{-1} [Eq. (27)]	$2u_1/\pi^{1/2}u_0$ [Eq. (28a)]	$u_0^{-1}\times(2u_1/\pi^{1/2}u_0)$
0.9999	0.010999	55.872	0.61454
0.999	0.034771	17.671	0.61443
0.99	0.10964	5.5972	0.61368
0.9	0.33662	1.8024	0.60671
0.8	0.45933	1.3043	0.59909
0.7	0.54075	1.0943	0.59176
0.6	0.59733	0.97926	0.58494
0.5	0.63487	0.91212	0.57907
0.4	0.65538	0.87727	0.57494
1/3[a]	0.65946	0.87028	0.57392
0.3	0.65337	0.87223	0.57425
0.2	0.64001	0.90866	0.58155
0.1	0.58693	1.0475	0.61482
0.01	0.42368	2.1738	0.92100

[a]Reference 8 obtained this result.

same numerical values for a given random walk. From the values in Tables V and VI and Eq. (26) it can be seen that u_0^{-1} is less than 10% greater in the upper bound although toward the two-dimensional limit the difference becomes somewhat larger. In the same way the coefficient of the time decaying correction term, given by $2u_1/u_0\pi^{1/2}$ [Eq. (26b)], is less than 20% smaller for the upper bound over the same range. Toward the two-dimensional limit the correction becomes somewhat larger. Thus, it suffices to use the lower bound topology, which is mathematically simpler.

Since the number of steps in time t is $n=\nu_{TOT}\,t$, where ν_{TOT} is the total frequency of steps, Eq. (26) can be employed [neglecting terms $\mathcal{O}(n^{-1})$ in Eq. (26b)] to give the time-dependent cage sampling function

$$S_{CAGE}(t)=\frac{\nu_{TOT}}{u_0}\,t\,(1+k_1\,t^{-1/2})\,, \tag{29}$$

where the constant coefficient k_1 of the correction term is

$$k_1=\frac{2u_1}{\pi^{1/2}u_0}\,\nu_{TOT}^{-1/2}\,. \tag{30}$$

In order to illustrate the behavior of the time-dependent nature of $S(t)$, several sets of walk parameters will be considered. The following calculations will employ the lower limit formulas and take $\nu_C=\nu_{C'}$, i.e., $C=C'$, since with these conditions all of the properties of three-dimensional topologies can be illustrated and a convenient closed form expression is available for u_0[20]:

$$u_{0\mathcal{L}}=U_{\mathcal{L}}(1,\,0)=\frac{1}{C}\,I[(L/C)^{1/2}]\,, \tag{31}$$

where $I(\alpha)$ is given by

$$I(\alpha)=4[(\gamma+1)^{1/2}-(\gamma-1)^{1/2}]K(k_2)K(k_3)/\alpha\pi^2\,, \tag{32a}$$

$$k_2=\tfrac{1}{2}[(\gamma-1)^{1/2}-(\gamma-3)^{1/2}][(\gamma+1)^{1/2}-(\gamma-1)^{1/2}]\,, \tag{32b}$$

$$k_3=\tfrac{1}{2}[(\gamma-1)^{1/2}+(\gamma-3)^{1/2}][(\gamma+1)^{1/2}-(\gamma-1)^{1/2}]\,, \tag{32c}$$

$$\gamma=(4+3\alpha^2)/\alpha^2\,, \tag{32d}$$

and where $K(k)$ is the complete elliptic integral of the first kind of modulus k. For example, consider a system with site-to-site hopping frequency $\nu_{INC}=10^{12}\ \mathrm{sec}^{-1}$. The on-chain frequency between supersites ν_L is typically (Sec. III. A) $10^7\ \mathrm{sec}^{-1}$. If the frequency of steps between adjacent chains is scaled down by $\sim 10^9$ from ν_{INC}, then the interchain cage stepping frequency will be of the order of $\nu_C\approx 10^3\ \mathrm{sec}^{-1}$. This results in a walk which is predominantly one-dimensional along a single chain, since from Eq. (24) it is seen that $L\approx 0.9999$ and $\nu_{TOT}\approx 10^7\ \mathrm{sec}^{-1}$. Using the values from Table V in Eqs. (27)–(30), the cage sampling function is $S(t)\approx 0.11t\times(1+18t^{-1/2})$, with t in units of μsec. The correction term $18t^{-1/2}$ is still half as large as unity at 1 msec and at times less than 10 μsec (equivalent to 100 steps) the correction term is much greater than one, making $S(t)\propto t^{1/2}$, which is the time-behavior characteristic of purely one-dimensional random walks [see Eq. (11)]. When confined to a linear chain, the exciton frequently revisits (nontrap) sites whereas even one off-chain step dramatically increases $S(t)$.

In the limit that the walk becomes strictly one-dimensional, L approaches unity, the coefficient u_0^{-1} of Eq. (26) goes to zero, and the coefficient of the $n^{-1/2}$ term of Eq. (26b) diverges. However, as seen in Table V, the product of these coefficients is a constant (~ 0.615), so that the time-dependent cage sampling function [Eqs. (29) and (30)] is given by $S(t)\approx 0.615\,\nu^{1/2}t^{1/2}$. This should be compared to the one-dimensional form $S(t)\approx 1.60\,\nu^{1/2}t^{1/2}$ from Eq. (11). The numerical factor of ~ 2.5 can be ascribed to the inappropriate application of the Tauberian theorem near the limit $L\to 1$, but the important point is that the functional forms are identical, indicating the reliability of the limiting behavior in this situation.

TABLE VI. Three-dimensional random walk sampling parameters for the upper bound (staggered lattice) topology (Fig. 3). The interchain step probabilities [Eq. (24)] C and C' have been set equal. $L+C+C'=1$.

Along-chain step probability L	u_0^{-1} [Eq. (27)]	$2u_1/\pi^{1/2}u_0$ [Eq. (28b)]	$u_0^{-1}\times(2u_1/\pi^{1/2}u_0)$
0.9999	0.0173	48.3	0.748
0.999	0.0367	16.7	0.611
0.99	0.114	5.20	0.593
0.9	0.349	1.65	0.576
0.8	0.477	1.19	0.565
0.7	0.565	0.984	0.556
0.6	0.629	0.869	0.546
0.5	0.675	0.797	0.538
0.4	0.708	0.749	0.531
1/3	0.7230	0.7278	0.5263
0.3	0.729	0.720	0.525
0.2	0.738	0.708	0.523
0.1	0.733	0.714	0.524
0.01	0.718	0.745	0.535

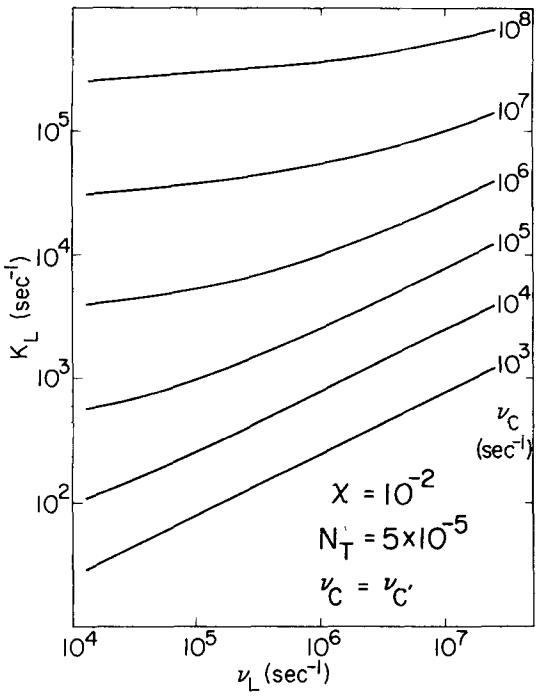

FIG. 4. The time-independent leading term of the trapping rate function K_L for a quasi-one-dimensional system is plotted as a function of the along-chain cage stepping frequency ν_L for several different interchain cage stepping frequencies ν_C. The scattering impurity concentration is 10^{-2} and the concentration of traps is 5×10^{-5}. K_L is much more strongly dependent on ν_L when $\nu_L \gg \nu_C$.

The trapping rate function is now obtained from the number of distinct lattice sites sampled in a time t. Equations (4), (24), and (27)–(30) may be combined to give the sampling function for distinct lattice sites

$$S(t) = (\chi^{-1} - 1)\,\frac{\nu_{TOT}}{u_0}\,t(1 + k_1 t^{-1/2}). \tag{33}$$

Using Eq. (1), the trapping rate function is found to be

$$K_L(t) = K_L + B_L\,t^{-1/2}\ , \tag{34}$$

where the time-independent parameters are

$$K_L = N_T(\chi^{-1} - 1)\,\frac{\nu_{TOT}}{u_0}\ , \tag{35}$$

$$B_L = \frac{k_1 K_L}{2} = \frac{N_T(\chi^{-1} - 1)\,\nu_{TOT}^{1/2}\,u_1}{\pi^{1/2}u_0^2}\ . \tag{36}$$

u_0 and u_1 must be chosen for the appropriate topology, and the microscopic details of the transport enter through the various parameters in Eqs. (33)–(36). If the second term is negligible, the localization rate function becomes a simple rate constant $K_L(t) = K_L$.

The time dependence of the trapping rate function given by Eq. (34) is a general consequence of the nature of random walks with three-dimensional topology. This functional dependence on time was employed by Soos and Powell in a study of singlet exciton trapping for a three-dimensional molecular lattice[15] with near-isotropic interactions. The model presented here also considers a random walk with a three-dimensional topology but this topology arises from consideration of scattering impurities in quasi-one-dimensional systems and leads to a different physical interpretation of the walk, which has several important consequences. First, as discussed above, this model does not evaluate a sampling function for a random walk between lattice sites, but rather for a random walk between supersites. The topology of the random walk may be three dimensional in nature even though the intermolecular interactions responsible for exciton migration are essentially one dimensional. Thus, the time dependence of the trapping rate predicted by Eq. (34) is expected for a variety of systems, not just those which have truly three-dimensional intermolecular interactions. Furthermore, a random walker on the three-dimensional superlattice associated with quasi-one-dimensional transport has a relatively low stepping frequency compared to the isotropic pure crystal case. This greatly enhances the importance of the $t^{-1/2}$ "correction" term [e.g., Eqs. (29) or (34)] especially for excitations with short lifetimes, regardless of the relative anisotropy of the random walk.

The behavior of the leading term of the trapping rate function K_L is illustrated in Figs. 4 and 5 for a range of values of ν_L and ν_C, the cage stepping frequencies along the chain and off the chain, respectively. The details of the calculation of these frequencies are left unspecified, although a constant value of the scattering impurity concentration $\chi = 10^{-2}$, is used for all curves, so the range of along-chain frequencies would represent variation in the physical parameters other than χ (see Sec. III. A). The trap concentration is $N_T = 5\times10^{-5}$. In Fig. 4 it can be seen that K_L has a much stronger dependence on ν_L when $\nu_L \gg \nu_C$, $\nu_{C'}$. In Fig. 5 a family of

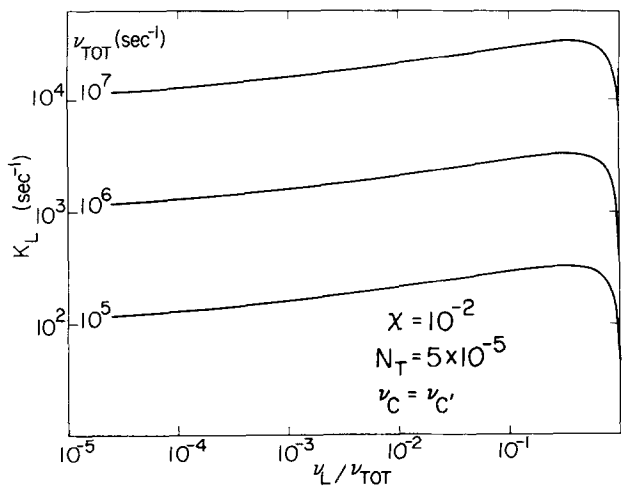

FIG. 5. The time-independent leading term of the trapping rate function K_L for a quasi-one-dimenstional system is plotted as a function of ν_L/ν_{TOT} (or L), the fraction of cage steps along the chain, for several values on the on-chain stepping frequency ν_L. The ratio L ranges from zero (the two-dimensional limit) to unity (the one-dimensional limit). The maximum trapping rate constant is obtained at $L = 1/3$, i.e., cage steps are equally probable in all three directions. Whe $L \to 1$, $K_L \to 0$, and the time-dependent term constitutes the entire trapping rate function.

curves of K_L vs ν_L/ν_{TOT} is displayed for various constant total stepping frequencies ν_{TOT}. As the walk changes from two dimensional ($\nu_L/\nu_{TOT} \to 0$) to nearly three dimensional, the value of K_L increases to a maximum at $\nu_L/\nu_{TOT} = 1/3$. At the one-dimensional limit ($\nu_L/\nu_{TOT} \to 1$), the value of K_L declines precipitously to a value of zero. In this situation the "correction" term $B_L t^{-1/2}$ constitutes the entire rate of trapping. Each subsequent curve represents a factor of 10 increase in K_L at every point since $K_L \propto \nu_{TOT}$. These calculations use Eq. (31) in (35). It can be seen that the trapping rate function has a complex dependence on all the physical parameters including the off-chain stepping frequencies. The mode of microscopic transport and the molecular parameters β, S, and T in combination with the mole fraction of scattering impurities χ enter into a straightforward evaluation of ν_L through Eqs. (6) or (10). However, since χ also enters directly into $K_L(t)$ through the cage size, the overall dependence on χ depends in turn on the relative magnitudes of ν_L and ν_C, $\nu_{C'}$. If $\nu_L \gg \nu_C$, $\nu_{C'}$, then from Eq. (35), $K_L(t) \propto (\chi^{-1}-1)^{1/2}$. This is the behavior of a one-dimensional random walk. In contrast, if $\nu_L \ll \nu_C, \nu_{C'}$, then $K_L(t) \propto (\chi^{-1}-1)$. In this limit the trapping rate increases linearly with cage size, and is independent of the along-chain cage stepping frequency [Eqs. (6) or (10)]. This behavior is illustrated in Fig. 6, a log–log plot of the parameter K_L vs χ for quasi-one-dimensional migration which is microscopically coherent with $\beta = 0.5$ cm^{-1}, $S = 32$ cm^{-1}, and the temperature 1.4°K. An analogous calculation could be performed for microscopically incoherent transport. The lowest curve represents the case where $\nu_L \approx 10^6$–10^7 sec$^{-1} \gg \nu_C = 10^3$ sec^{-1}, and the expected slope 0.5 is observed. The top curve illustrates the other limit, i.e., $\nu_L \approx 10^4$ sec$^{-1} \ll \nu_C = 10^7$ sec^{-1}. This curve has a slope of 0.9, which approaches the limiting value of unity. Thus, the concentration dependence reveals the extent of deviation from a one-dimensional topology.

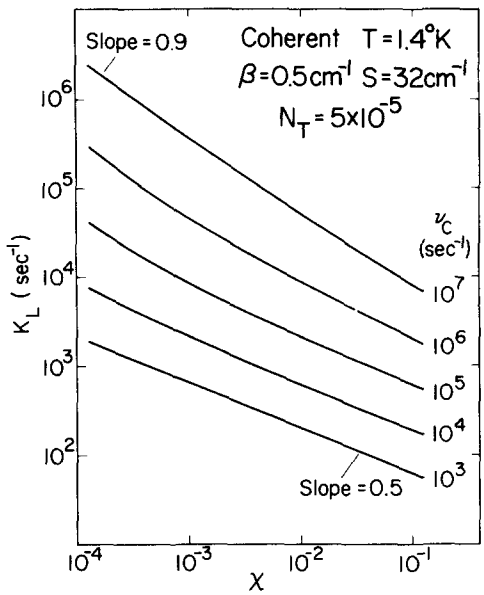

FIG. 6. The effect of scattering impurity concentration on the time-independent leading term of the trapping rate function K_L for a quasi-one-dimensional system is illustrated for several values of interchain cage stepping frequency $\nu_C = \nu_{C'}$. A hypothetical molecular system is used for the entire figure, having coherent exciton migration at 1.4 °K with an intermolecular interaction matrix element $\beta = 0.5$ cm^{-1}. The scattering impurities are $S = 32.0$ cm^{-1} in energy above the center of the band. The concentration of traps in 5×10^{-5}. When the frequency of steps along the linear chain ν_L is much greater than the interchain cage stepping frequency ν_C, the slope of one-half results, demonstrating the essentially one-dimensional nature of this system (e.g., in this system when $\chi = 0.1$ and $\nu_C = 10^3$ sec^{-1}). In the opposite case $\nu_L \ll \nu_C$ (e.g. $\chi = 10^{-4}$, $\nu_C = 10^7$ sec^{-1}), the slope is approaching unity indicating the multidimensional nature of that system.

The dependence of $K_L(t)$ on the other parameters of the system—the mode of migration, β, S, and T—also depends in turn on the relative magnitudes of ν_L and ν_C, $\nu_{C'}$ as it did for χ. However, these parameters enter into the calculation only through the stepping frequency ν_L. The results of typical calculations are tabulated along with the time $t_{10\%}$, at which the correction term $B_L t^{-1/2}$ is down to 10% of the leading term K_L. Table VII lists the values of K_L and B_L for coherent migration along chain at a temperature of 1.4°K with $\beta = 10$ cm^{-1}, $S/\beta = 33$, and $N_T = 5 \times 10^{-5}$. Table VIII gives the values of K_L and B_L for incoherent migration along chain, also with $S/\beta = 33$, but the microscopic hopping time $\nu_{INC}^{-1} = 1$ psec. Only when $\nu_C t \gg 1$ can the correction term be neglected. This must be considered when formulating the trapping rate function, for if $B_L t^{-1/2}$ is negligible, the results are simplified. In addition, both K_L and B_L have a linear dependence on the concentration of trap sites N_T. Therefore, N_T affects only the overall rate of trapping, not the relative importance of the two terms in $K_L(t)$.

The population equations can now be solved. Both the lower and upper bound three-dimensional lattices yield the same form for the localization rate function, $K_L(t) = K_L + B_L t^{-1/2}$. The solutions are obtained by inserting this form into Eq. (3) to yield

$$E(t) = \exp[-(K_E + K_L)t - 2B_L t^{1/2}], \tag{37a}$$

$$T(t) = \exp(-K_T t)\left[\frac{K_L}{K_L + K_E - K_T}\{1 - \exp[-(K_L + K_E - K_T)t - 2B_L t^{1/2}]\}\right.$$
$$+\left(\frac{B_L^2 \pi}{K_L + K_E - K_T}\right)^{1/2} \exp[B_L^2/(K_L + K_E - K_T)]\left(1 - \frac{K_L}{K_L + K_E - K_T}\right)$$
$$\left.\times\left(\operatorname{erf}\left\{[(K_L + K_E - K_T)t]^{1/2} + \frac{B_L}{(K_E - K_T + K_L)^{1/2}}\right\} - \operatorname{erf}\left[\frac{B_L}{(K_E - K_T + K_L)^{1/2}}\right]\right)\right], \tag{37b}$$

TABLE VII. Coefficients of the quasi-one-dimensional trapping function $K_L(t) = K_L + B_L t^{-1/2}$. In this example, the exciton migration along chain is coherent at 1.4 °K, with $\beta = 10$ cm^{-1} and $S/\beta = 33$. The trap concentration is 5×10^{-5}. The time at which $B_L t^{-1/2} = 10\%\ K_L$ is defined at $t_{10\%}$. Each block of numbers is, in descending order, K_L(sec^{-1}), B_L(sec$^{-1/2}$), $t_{10\%}$.

Interchain stepping frequency $\nu_C = \nu_{C'}$ (sec^{-1})	Impurity concentration 10^{-1}	10^{-2}	10^{-3}
10^6	3.6×10^3	1.3×10^4	6.5×10^4
	0.71	3.0	23
	3.9 μsec	5.3 μsec	12 μsec
10^4	350	1.2×10^3	3.7×10^3
	0.69	2.3	7.4
	0.39 msec	0.37 msec	0.40 msec
10^2	35	120	360
	0.69	2.3	7.2
	39 msec	37 msec	40 msec
ν_L (sec^{-1})[a]	2.5×10^7	2.3×10^6	2.2×10^5

[a]The along-chain cage stepping frequency for each impurity concentration (see Table I).

where erf(x) is the error function of argument x. If the correction term is negligible over the time domain of the walk, then the solutions become

$$E(t) = \exp[-(K_L + K_E)\,t]\ , \tag{38a}$$

$$T(t) = \exp(-K_T\,t)\,\frac{K_L}{K_L + K_E - K_T} \times\{1 - \exp[-(K_L + K_E - K_T)\,t]\}\ . \tag{38b}$$

Small deviations from strictly one-dimensional transport can have a dramatic effect on exciton trapping. This effect is illustrated in Fig. 7. For all curves in this example, exciton transport along the linear chain is taken to be incoherent with $\nu_{INC}^{-1} = 1$ psec and $S/\beta = 100$. The impurity concentration is 10^{-2}, and the trap concentration is 5×10^{-5}. The exciton and trap decay rates are 50 and 20 sec^{-1}, respectively. The bottom curve uses the strictly one-dimensional formula [Eq. (20b)]. Here, $A_{INCOH} = 5.6$ sec$^{-1/2}$ (see Table IV). In the top three curves small interchain step frequencies are included, i.e., $\nu_C = \nu_{C'} = 10^6$, 10^4, and 10^3 sec^{-1}, respectively, and Eq. (38b) is employed. Even cross-chain stepping frequencies which are 10^{-9} of on-chain site-to-site frequencies have a large effect. The integrated trap population which is proportional to the trap intensity under steady state conditions is also very sensitive to the small degree of interchain exciton transport. This figure should be compared to Fig. 1. It can be seen that very small interactions between adjacent chains can produce the same effects as variations in the parameters associated with a strictly one-dimensional random walk. In Fig. 7, as the trapping parameter decreases, a more gradual and later buildup to maximum is observed, and the maximum is broader. The total integrated populations also decrease. Neglect-

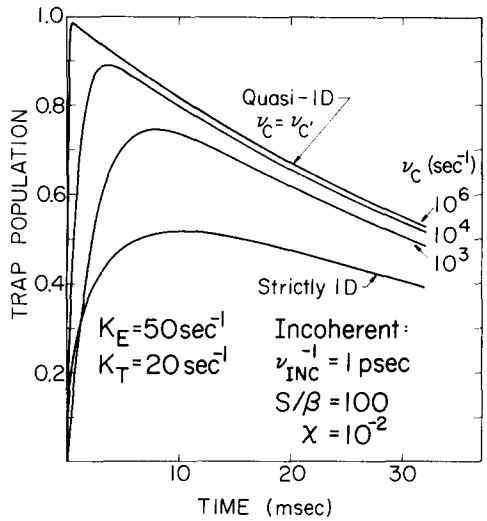

FIG. 7. The effect of very slow cross-chain transport on the time-dependence of the trap population following impulse excitation of the exciton band is displayed. The bottom curve is for strictly one-dimensional transport with a site-to-site incoherent stepping time $\nu_{INC}^{-1} = 1$ psec. The exciton and trap decay rate constants (inverse lifetime) are 50 and 20 sec^{-1}, respectively. The scattering impurity and trap concentrations are 10^{-2} and 5×10^{-5}, respectively. The other three curves are calculated using an identical set of parameters but also include varying degrees of cross-chain stepping, i.e., 10^3, 10^4, and 10^6 sec^{-1} moving from bottom to top. These cross-chain frequencies are 6 to 9 orders of magnitude smaller than the on chain site-to-site stepping frequency, yet have a very large influence.

TABLE VIII. Coefficients of the quasi-one-dimensional trapping function $K_L(t) = K_L + B_L t^{1/2}$. The exciton migration along chain is incoherent with a microscopic hopping time $\nu_{INC}^{-1} = 1$ psec, $S/\beta = 33$, and the trap concentration is 5×10^{-5}. The time at which $B_L t^{-1/2} = 10\%\ K_L$ is defined as $t_{10\%}$. Each block of three numbers is, in descending order, K_L (sec^{-1}), B_L (sec$^{-1/2}$), $t_{10\%}$.

Interchain stepping frequency $\nu_C = \nu_{C'}$ (sec^{-1})	Impurity concentration 10^{-1}	10^{-2}	10^{-3}
10^6	9.9×10^3	3.1×10^4	8.3×10^4
	2.0	6.4	23
	3.9 μsec	4.2 μsec	7.8 μsec
10^4	990	$3.1\cdot10^3$	$5.9\cdot10^3$
	2.0	6.1	12
	0.39 msec	0.39 msec	0.39 msec
10^2	99	310	580
	2.0	6.1	11
	39 msec	39 msec	39 msec
ν_L (sec^{-1})[a]	2.0×10^8	1.6×10^7	5.6×10^5[b]

[a]The along-chain cage stepping frequency for each impurity concentration (see Table II).
[b]This result is approximate. See the discussion surrounding Eq. (8).

ing the correction term $B_L t^{-1/2}$ is a reasonable assumption for this time domain (see Table VIII). In Fig. 8(A), the lowest of the three quasi-one-dimensional trapping curves of Fig. 7, where $\nu_C = 10^3$ sec^{-1}, is displayed with and without the correction term. In contrast, Fig. 8(B) uses the same random walk—trapping parameters, but involves a quite different time domain by virtue of much faster exciton and trap decay rate constants, now 5×10^6 and 2×10^6 sec^{-1}, respectively. In this time domain the correction term dominates the leading term. By itself, the leading term accounts for only ~ 5% of the total integrated trap population. This figure clearly demonstrates that the time domain determines the effective functional form of $K_L(t)$. In this last example, a much better description is probably offered by the strictly one-dimensional random walk of Sec. III. B.

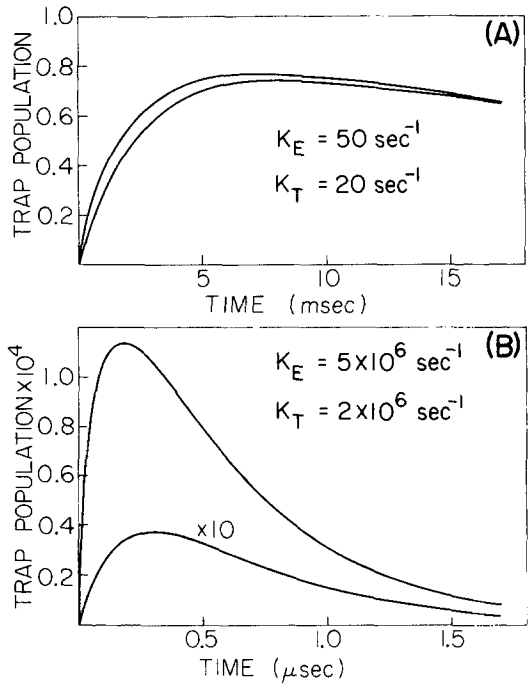

FIG. 8. The calculated trap population for a quasi-one-dimensional system is plotted as a function of time. In the upper curves of both figures the $B_L t^{-1/2}$ term was included [i.e., Eq. (34a) was used] and in the lower curves of both figures this term was neglected [i.e., Eq. (34b) was used]. The system is near the one-dimensional limit, with $\nu_L = 2\times10^6$ sec^{-1} and $\nu_C = \nu_C' = 10^3$ sec^{-1}. The scattering impurity concentration is 10^{-2} and the concentration of traps is 5×10^{-5}. Using Eqs. (35) and (36), this yields $K_L = 340$ sec^{-1} and $B_L = 2.2$ sec$^{-1/2}$. (A) The exciton and trap decay constants are 50 and 20 sec^{-1}, respectively. In this situation, the inclusion of the $B_L t^{-1/2}$ term causes only a small change in the maximum and integrated populations, since the long time domain ensures that very many cage steps will occur. This term is only 10% of the leading term K_L at 3.9 msec. (B) For the same system, the exciton and trap decay constants are set 10^5 times faster, i.e., 5×10^6 and 2×10^6 sec^{-1}, respectively. In this situation, the "correction" term by far dominates the leading term, accounting for 95% of the integrated population, since the short time domain permits relatively few cage steps.

IV. TRAPPING, TRANSPORT, AND THE MEAN-SQUARE DISPLACEMENT

In the previous sections the effect of very small off-chain interactions on the trapping rate was discussed. The trapping rate for a quasi-one-dimensional system can behave as if it had a two- or three-dimensional topology on the superlattice. However, the transport of excitons as measured by the RMS displacement along the chain as well as in the two orthogonal directions will remain predominantly one dimensional. For example, consider the mean-square displacements of a macroscopically random walking exciton on an idealized simple cubic topology of uniform cages, as in Sec. III. C,

$$\langle D_x^2\rangle = \nu_x t\overline{d_x^2} = \nu_x t(\chi^{-1}-1)^2a^2 ,$$
$$\langle D_y^2\rangle = \nu_y t\overline{d_y^2} = \nu_y t a^2 ,$$
$$\langle D_z^2\rangle = \nu_z t\overline{d_z^2} = \nu_z t a^2 , \qquad (39)$$

where $\langle D_i^2\rangle$ is the total mean-square displacement, ν_i is the stepping frequency, and $\overline{d_i^2}$ the mean-square displacement per step in the ith direction. The mean step size between adjacent chains is of the order of one lattice site spacing a. In contrast, the mean step size along the chain is the number of lattice sites in a cage times a, $(\chi^{-1}-1)a$. If the trapping, and hence the sampling of cages, behaved completely isotropically, then all the stepping frequencies would be equal $\nu_x = \nu_y = \nu_z \equiv \nu$. The RMS displacement in three-dimensional space would be given for the ith direction by $D_{i\,\mathrm{rms}} \equiv (\langle D_i^2\rangle)^{1/2}$, so that the vector displacement would be

$$\mathbf{D}_{\mathrm{RMS}} = (\nu t)^{1/2} a[(\chi^{-1}-1)\mathbf{i}+\mathbf{j}+\mathbf{k}] , \qquad (40)$$

where the above definition of D_{RMS} has been employed in combination with Eq. (39). The usual definition of the unit vectors $\mathbf{i}$, $\mathbf{j}$, and $\mathbf{k}$ has also been used. This displacement describes a three-dimensional Gaussian probability distribution which would appear to be a long, thin, tapering cylinder along the one-dimensional direction. This basically one-dimensional displacement of excitons occurs for a system whose trapping properties behave as if its topology were isotropically three dimensional. Therefore, in real quasi-one-dimensional systems, scattering impurities and very small interactions between adjacent chains can cause the trapping properties to follow a topology which may be quite unrelated to the transport topology of excitons as measured by their displacements in physical space.

V. SUMMARY

In order to closely model real systems with almost one-dimensional energy transport, the effects of low concentration scattering impurities and small deviations from one dimensionality on exciton migration and trapping in molecular crystals were considered. The trapping rate function has the same dependence on time and on impurity concentration for microscopically coherent or incoherent excitons. In the strictly one-dimensional limit, the trapping rate function is always time dependent. Small multidimensional interactions change the effective trapping topology. At short times, a time-dependent trapping rate function results. If the multidimensional interactions are sufficient to produce

a very large number of off-chain steps during the exciton lifetime, then the trapping rate function tends toward a constant and trapping appears as if transport were three dimensional. Regardless of the apparent dimensionality of trapping, the exciton mean-square displacement remains one dimensional. However, trapping is greatly increased by even a small amount of multidimensional transport.

The model provides a way to examine the dimensionality of exciton transport and the rate of cross-chain steps through the scattering impurity concentration dependence of exciton trapping. Detailed analysis of time-dependent trapping data can provide direct information on the macroscopic rate of exciton transport. In a subsequent publication,[14] an experimental study of triplet exciton trapping in 1, 2, 4, 5-tetrachlorobenzene (h_2-TCB) doped with deuterated scattering impurities will be presented. In these systems, transport is clearly dominated by exciton–impurity scattering. The $\chi^{-1/2}$ concentration dependence predicted here is observed. TCB is shown to be overwhelmingly one dimensional with a cross-chain stepping frequency less than 5×10^3 $\sec^{-1}$. Thus, the model provides a framework for the investigation of transport topology, small intermolecular interactions, and macroscopic exciton transport.

ACKNOWLEDGMENTS

This work was supported by the National Science Foundation, Division of Materials Research grant DMR 76-22019. In addition, acknowledgment is made to the donors of the Petroleum Research Fund, administered by the American Chemical Society, for partial support of this research.

APPENDIX A. THE TRAPPING RATE FUNCTION

The relationship between the trapping rate function $K_L(t)$ and the sampling function $S(t)$ is obtained from a simple consideration of exciton population dynamics. The exciton population at any time is the product of the probability of not having decayed $e^{-K_E t}$ and the probability of not having trapped. The probability of *not* sampling a trap site is $(1-N_T)^{S(t)}$, the normalized number of ways of sampling $S(t)$ *nontrap* sites. Thus, the exciton population is

$$E(t) = e^{-K_E t}(1-N_T)^{S(t)} \tag{A1a}$$

$$= \exp\left[-K_E t - \ln\left(\frac{1}{1-N_T}\right) S(t)\right]. \tag{A1b}$$

Since the time evolution of this population is also described by the rate equation

$$\dot{E}(t) = -K_E E(t) - K_L(t) E(t)\ , \tag{A2}$$

Eq. (A1b) can be substituted into Eq. (A2) and the identification

$$K_L(t) = \ln\left(\frac{1}{1-N_T}\right)\dot{S}(t) \tag{A3}$$

is made.

APPENDIX B. THE RANDOM WALK FUNCTIONS OF THE THREE-DIMENSIONAL STAGGERED TOPOLOGY

The staggered three-dimensional arrangement of quasi-one-dimensional chains generates an upper limit to the sampling function $S(t)$. This topology is illustrated in Fig. 3. A step from any supersite occurs to an adjacent supersite which can be in one of three classes of distinct positions. The stepping probability of each class is given in Table IX. The total probability of a class is given by the stepping frequencies of the random walk [Eq. (24) Sec. III. C] and is defined as the probability of a step to a position times the number of such positions. Thus, $L = 2P_L$, $C = 4P_C$, and $C' = 4P_{C'}$.

A random step occurs to any one of 12 supersites accessible by a single step. The first class of supersites consists of the two neighbors along the linear chain. The second class will be the four neighbors on the adjacent chains. They are centered on the impurity sites which bound the initial supersite. Both classes of super sites lie in the initial plane. In this arrangement, each impurity site of a chain is centered relative to the centers of the supersites on the two neighboring chains so that no two impurity sites are adjacent in the plane [see Fig. 3(A)]. The third class, consisting of two subclasses, can be visualized from Fig. 3(B), a cross section containing impurity sites (black squares) and perpendicular to the chains. Relative to the central white square in the array the first subclass consists of the two white squares staggered above and below that square. The supersites represented by these squares and the central square all have impurities in the planes one-half supersite from the plane in the figure; thus, a step to this subclass is weighted by the full probability of this step $P_{C'}$. The remaining four supersites, whose impurities lie in the plane of the cross section, are represented by the black squares to the left and right. Steps to these four supersites are weighted by one-half probability $\frac{1}{2}P_{C'}$, because each has an "overlap" with the initial supersite of $\frac{1}{2}$.

The structure function for this topology is obtained in the standard way[17(a)] from these positions and individual probabilities

$$\begin{aligned}\lambda_u(\phi_1,\phi_2,\phi_3) = {} & P_L(\exp(i\phi_1)+\exp(-i\phi_1)) + P_C(\exp[i(\phi_1/2+\phi_2)]+\exp[i(\phi_1/2-\phi_2)] \\ & +\exp[i(-\phi_1/2+\phi_2)]+\exp[i(-\phi_1/2-\phi_2)]) + P_{C'}(\exp[i(\phi_2/2-\phi_3)] \\ & +\exp[i(-\phi_2/2+\phi_3)]) + \tfrac{1}{2}P_{C'}(\exp[i(\phi_1/2+\phi_2/2+\phi_3)]+\exp[i(-\phi_1/2+\phi_2/2+\phi_3)] \\ & +\exp[i(\phi_1/2-\phi_2/2-\phi_3)]+\exp[i(-\phi_1/2-\phi_2/2-\phi_3)])\ .\end{aligned} \tag{B1}$$

TABLE IX. The stepping probability for each class.

Position class	Position	Individual probability	Class total probability
Original chain: (1D direction)	$(\pm 1, 0, 0)$	P_L	L
Adjacent chain: (in plane)	$(\pm\frac{1}{2}, \pm 1, 0)$	P_C	C
Adjacent chain: (out of plane)	$(0, -\frac{1}{2}, 1)$	$P_{C'}$	C'
	$(0, \frac{1}{2}, -1)$		
	$(\pm\frac{1}{2}, \frac{1}{2}, 1)$	$\frac{1}{2}P_{C'}$	
	$(\pm\frac{1}{2}, -\frac{1}{2}, -1)$		

Using several trigonometric identities and substituting the group probabilities L, C, and C' for the individual step probabilities, the result is obtained in its most convenient form for the numerical evaluation of the Green's function $U(1, 0)$:

$$\lambda_{\mathfrak{u}}(\phi_1, \phi_2, \phi_3) = L\cos\phi_1 + C\cos\left(\frac{\phi_1}{2}\right)\cos\phi_2 + \frac{1}{2}C'\left[\cos\left(\frac{\phi_2}{2} - \phi_3\right) + \cos\frac{\phi_1}{2}\cos\left(\frac{\phi_2}{2} + \phi_3\right)\right]. \tag{B2}$$

The other important quantity to be calculated from the structure function is the correction term in $S(t)$ [Eq. (28b)]. Montroll showed that the Green's function could be expanded in z as $z \to 1$:

$$U(z, 0) = u_0 - u_1(1-z)^{1/2} + \mathcal{O}(1-z). \tag{B3}$$

The coefficient u_1 may be deduced from the behavior of $\lambda(\phi_1, \phi_2, \phi_3)$ near the origin [see Ref. 17(a), p. 181]. Equation (B2) may be rewritten using a trigonometric identity as

$$\lambda_{\mathfrak{u}}(\phi_1, \phi_2, \phi_3) = L\cos\phi_1 + C\cos\frac{\phi_1}{2}\cos\phi_2 + C'\left(\cos^2\frac{\phi_1}{4}\cos\frac{\phi_2}{2}\cos\phi_3 + \sin^2\frac{\phi_1}{4}\sin\frac{\phi_2}{2}\sin\phi_3\right). \tag{B4}$$

Expanding this form for ϕ near the origin yields

$$\lambda_{\mathfrak{u}}(\phi_1, \phi_2, \phi_3) \approx 1 - \frac{1}{2}\left[\left(L + \frac{C}{4} + \frac{C'}{8}\right)\phi_1^2 + \left(C + \frac{C'}{4}\right)\phi_2^2 + C'\phi_3^2 + \mathcal{O}(\phi^4)\right], \tag{B5}$$

and using Montroll's method the identification can be made

$$u_{1\mathfrak{u}} = \left[2\pi^2\left(L + \frac{C}{4} + \frac{C'}{8}\right)\left(C + \frac{C'}{4}\right)C'\right]^{-1/2}. \tag{B6}$$

APPENDIX C. THE TWO-DIMENSIONAL LIMIT IN QUASI-ONE-DIMENSIONAL TRANSPORT

In quasi-one-dimensional systems with interchain interactions in only one dimension, the exciton migrates on a plane. Here we will consider only the lower bound topology in which the scattering impurities are aligned in the plane as in Fig. 2(A). This forms a "square" topology because steps occur either to cage position $(\pm 1, 0)$ along the one-dimensional direction or to cage position $(0, \pm 1)$ in the orthogonal direction. This idealized lattice provides a lower limit for the two-dimensional sampling of new lattice sites, in analogy to Sec. III. C. The sampling function can be readily obtained for this lattice once the two stepping frequencies are specified. These quantities provide the relative stepping probabilities and the total stepping frequency

$$\begin{aligned} &1D \text{ direction:} && L = P(1, 0) + P(-1, 0) = \nu_L/\nu_{\mathrm{TOT}}, \\ &\text{Interchain:} && C = P(0, 1) + P(0, -1) = \nu_C/\nu_{\mathrm{TOT}}, \\ & && \nu_{\mathrm{TOT}} = \nu_L + \nu_C . \end{aligned} \tag{C1}$$

The stepping frequency in one dimension ν_L is taken from Eq. (6) or (10) depending on the microscopic mode of transport.

The trapping rate can be calculated for arbitrary ν_C. Montroll showed by use of a Tauberian theorem that the number of distinct sites sampled after n steps $S(n)$ can be obtained in the asymptotic limit of large n from the behavior of the random walk Green's function $U(z, 0)$ as $z \to 1$:

$$U(z, 0) = \frac{1}{\pi z(LC)^{1/2}}\left[\frac{1}{2}\ln\frac{2^6 LCz^2}{(1-z)(1+z)} + \mathcal{O}(1-z)\right], \tag{C2}$$

where L and C are the relative step probabilities in the two directions. He obtained $S(n)$ in the special case that $L = C$,[8] an isotropic two-dimensional walk. In what follows, a generalization for $L \neq C$ is presented. First, we must use the relationship for $\Delta(z)$, the generating function of the number of additional distinct lattice sites sampled after each step,

$$\Delta(z) = \frac{z}{(1-z)U(z, 0)} . \tag{C3}$$

We find then that

$$\Delta(z) = 2\pi(LC)^{1/2}z^2/[-(1-z)\ln(1-z) - (1-z)\ln(1+z) + 2(1-z)\ln z + (1-z)\ln LC + 6(1-z)\ln 2 + 2(1-z)\mathcal{O}(1-z)]. \tag{C4}$$

To use the Tauberian theorem the asymptotic behavior of $\Delta(z)$ as $z \to 1$ is required. Making the substitution $e^{-y} \equiv z$, then as $z \to 1$, $y \to 0$ so that $1 - z \sim y$. Thus,

$$\Delta(z) \sim 2\pi(LC)^{1/2}(1-y)^2/[-y\ln y - y\ln(2-y) + 2y\ln(1-y) + y\ln LC + 6y\ln 2 + 2y\mathcal{O}(y)] \tag{C5}$$

as $y \to 0$ (equivalent to $z \to 1$). This can be rearranged to give

$$\Delta(z) \sim \left(\frac{2\pi}{y}\right)(LC)^{1/2}(1-y)^2/[\ln(1/y) - \ln(2-y) + 2\ln(1-y) + \ln LC + 6\ln 2 + 2\mathcal{O}(y)]. \tag{C6}$$

Finally, in the limit $y \to 0$, the third and sixth terms of the denominator vanish to give

$$\Delta(z) \sim \left(\frac{2\pi}{y}\right)(LC)^{1/2}/[\ln(1/y) + \ln LC + 5\ln 2] \tag{C7}$$

as $z \to 1$. Applying the Tauberian theorem, we choose (with $x \equiv y^{-1}$)

$$L(x) = \frac{2\pi(LC)^{1/2}}{\ln(2^5 LCx)} , \quad \sigma = 1 , \tag{C8}$$

so that $S(n) \sim n^{\sigma} L(n)$ and the generalized result is

$$S(n) = \frac{2\pi(LC)^{1/2} n}{\ln(2^5 LCn)} . \tag{C9}$$

This is the central result for the two-dimensional random walk which applies if n is not small. The number of steps in time t is $n = \nu_{\mathrm{TOT}} t$. Recalling that each cage sampled contains $l = (\chi^{-1} - 1)$ sites, all of which are sampled, the site sampling function is [see Eq. (4)]

$$S(t) = (\chi^{-1} - 1) \frac{2\pi(\nu_L \nu_C)^{1/2} t}{\ln(2^5 \nu_L \nu_C t/\nu_{\mathrm{TOT}})} . \tag{C10}$$

Using Eq. (1), the localization rate per unit population is found to be

$$K_L(t) = N_T(\chi^{-1} - 1) \frac{2\pi(\nu_L \nu_C)^{1/2}}{\ln(2^5 \nu_L \nu_C t/\nu_{\mathrm{TOT}})} \times [1 - 1/\ln(2^5 \nu_L \nu_C t/\nu_{\mathrm{TOT}})] . \tag{C11}$$

The two-dimensional result is more complicated than either the one- or three-dimensional result. Equation (C.11) can be substituted into Eq. (3), and while an analytical expression is not available, the time dependence of trap populations in this special limit can be obtained by numerical integration.

[1] A. J. Berlinsky, Contemp. Phys. **17**, 331 (1976); *Low-Dimensional Cooperative Phenomena*, edited by H. J. Keller (Plenum, New York, 1975); *Chemistry and Physics of One-Dimensional Metals*, edited by H. J. Keller (Plenum, New York, 1977); Abstracts of the Eighth Molecular Crystal Symposium, Santa Barbara, California (1977).

[2] J. Frenkel, Phys. Rev. **37**, 17 (1931); **37**, 1276 (1931); A. S. Davydov, *Theory of Molecular Excitons* (Plenum, New York, 1971); T. Holstein, Ann. Phys. (NY) **8**, 325 (1959); **8**, 343 (1959); Y. Toyozawa, Prog. Theor. Phys. **20**, 53 (1958); R. Reineker and H. Haken, Z. Phys. **250**, 300 (1972); H. Haken and P. Reineker, Z. Phys. **249**, 253 (1972); V. M. Kenkre and R. S. Knox, Phys. Rev. B **9**, 5279 (1974); Phys. Rev. Lett. **33**, 804 (1974); M. Grover and R. Silbey, J. Chem. Phys. **52**, 2099 (1970); **54**, 4843 (1971); R. W. Munn and W. Siebrand, J. Chem. Phys. **52**, 47 (1970); R. W. Munn, J. Chem. Phys. **52**, 64 (1970); J. M. Schurr, Mol. Phys. **27**, 357 (1974); H. Sumi and Y. Toyozawa, J. Phys. Soc. Jpn. **31**, 342 (1971); D. R. Yarkony and R. S. Silbey, J. Chem. Phys. **65**, 1042 (1976); **67**, 5818 (1977); C. B. Harris, J. Chem. Phys. **67**, 5607 (1977); R. M. Hochstrasser and J. D. Whiteman, J. Chem. Phys. **56**, 5945 (1972); A. H. Francis and C. B. Harris, Chem. Phys. Lett. **9**, 181, 188 (1971); A. H. Francis and C. B. Harris, J. Chem. Phys. **57**, 1050 (1972); D. D. Dlott and M. D. Fayer, Chem. Phys. Lett. **41**, 305 (1976); D. M. Burland, D. E. Cooper, M. D. Fayer, and C. R. Gochanour, Chem. Phys. Lett. **52**, 279 (1977); S. D. Woodruff and R. Kopelman, Chem. Phys. **22**, 1 (1977); D. E. Cooper and M. D. Fayer, J. Chem. Phys. **68**, 229 (1978); B. J. Botter, A. I. M. Dicker, and J. J. Schmidt, Mol. Phys. (in press).

[3] V. L. Broude and E. I. Rashba, Riz, Tverd. Tela **3**, 1941 (1961) [Sov. Phys. Solid State **3**, 1415 (1962)]; E. I. Rashba, Fiz. Tverd. Tela **5**, 1040 (1963) [Sov. Phys. Solid State **5**, 757 (1963)]; V. L. Broude and S. M. Kochubei, Fiz. Tverd. Tela **6**, 354 (1964) [Sov. Phys. Solid State **6**, 285 (1964)]; M. D. Fayer and C. B. Harris, Chem. Phys. Lett. **25**, 149 (1974); R. C. Powell and R. G. Kepler, Phys. Rev. Lett. 22 22, 639 (1969); R. C. Powell, Phys. Rev. B **4**, 628 (1971); R. C. Powell, J. Chem. Phys. **58**, 920 (1973); R. E. Merrifiled, J. Chem. Phys. **38**, 920 (1962); M. D. Fayer and C. B. Harris, Phys. Rev. B **9**, 748 (1974); D. D. Dlott and M. D. Fayer, Chem. Phys. Lett. **41**, 305 (1976); M. D. Fayer and C. R. Gochanour, J. Chem. Phys. **65**, 2472 (1976); R. M. Pearlstein, J. Chem. Phys. **56**, 2431 (1972); R. P. Hemenger, R. M. Pearsltein, and K. Lakatos-Lindenberg, J. Math. Phys. **13**, 1057 (1972); R. P. Hemenger and R. M. Pearlstein, Chem. Phys. **2**, 424 (1973); R. P. Hemenger, K. Lakatos-Lindenberg, and R. M. Pearlstein, J. Chem. Phys. **60**, 3271 (1974).

[4] D. D. Dlott, M. D. Fayer, and R. D. Wieting, J. Chem. Phys. **67**, 3803 (1977).

[5] G. F. Koster and J. C. Slater, Phys. Rev. **95**, 1167 (1954); **96**, 1208 (1954).

[6] D. M. Burland, V. Konzelmann, and R. M. Macfarlane, J. Chem. Phys. **67**, 1926 (1977).

[7] D. A. Zwemer and C. B. Harris, J. Chem. Phys. **68**, 2184 (1978).

[8] E. W. Montroll, Proc. Symp. Appl. Math. Am. Math. Soc. **16**, 193 (1964).

[9] (a) R. C. Powell, Phys. Rev. B **2**, 1159 (1970); **4**, 628 (1971); R. C. Powell and Z. G. Soos, J. Lumin. **11**, 1 (1975); (b) R. M. Shelby, A. H. Zewail, and C. B. Harris, J. Chem. Phys. **64**, 3192 (1976); W. Guettler, J. O. von Schuetz, and H. C. Wolf. Chem. Phvs. **24**. 159 (1977).

[10] R. M. Pearlstein, J. Chem. Phys. **56**, 2431 (1972); R. P. Hemenger, R. M. Pearslstein, and K. Lakatos-Lindenberg, J. Math. Phys. **13**, 1056 (1972); R. P. Hemenger and R. M. Pearlstein, Chem. Phys. **2**, 424 (1973); R. P. Hemenger, K. Lakatos-Lindenberg, and R. M. Pearlstein, J. Chem. Phys. **60**, 3271 (1974).

[11] V. M. Kenkre and R. S. Knox, Phys. Rev. B **9**, 5279 (1974); Phys. Rev. Lett. **33**, 804 (1974).

[12] M. Grover and R. Silbey, J. Chem. Phys. **52**, 2099 (1970); **54**, 4843 (1971).

[13] V. K. Shante and S. Kirkpatrick, Adv. Phys. **20**, 235 (1971); J. M. Ziman, J. Phys. C **1**, 1532 (1968); T. P. Eggarter and M. H. Cohen, Phys. Rev. Lett. **25**, 807 (1970); **27**, 129 (1971); J. Jortner and M. H. Cohen, J. Chem. Phys. **55**, 5380 (1971); H. K. Hong and R. Kopelman, Phys. Rev. Lett. **25**, 1030 (1970); J. Chem. Phys. **55**, 724 (1971); R. Kopelman, E. M. Monberg, F. W. Ochs, and P. N. Prasad, Phys. Rev. Lett. **34**, 1506 (1975); R. Kopelman, "Radiationless Processes in Molecules and Condensed Phases," in *Topics in Applied Physics*, edited by Francis K. Fong (Springer, New York, 1976), Vol. 15; J. Hoshen and R. Kopelman, J. Chem. Phys. **65**, 2817 (1976); J. Klafter and J. Jortner, Chem. Phys. Lett. **49**, 410 (1977); **50**, 202 (1977).

[14] D. D. Dlott, M. D. Fayer, and R. D. Wieting, J. Chem. Phys. (to be published).

[15] Z. G. Soos and R. C. Powell, Phys. Rev. B **6**, 4035 (1972).

[16] M. D. Fayer and C. B. Harris, Chem. Phys. Lett. **25**, 149 (1974); H. C. Brenner, J. C. Brock, M. D. Fayer, and C. B. Harris, Chem. Phys. Lett. **33**, 471 (1975).

[17] E. W. Montroll, J. Math. Phys. (a) **6**, 167 (1965); (b) **10**, 753 (1969).

[18] M. D. Fayer and C. B. Harris, Phys. Rev. B **9**, 748 (1974); **12**, 1784 (1974).

[19] V. M. Kenkre and R. S. Knox, Phys. Rev. Lett. **33**, 803 (1974).

[20] E. W. Montroll, *Proceedings of the* 3rd *Berkeley Symposium on Mathematical Statistics and Probability*, (Univeristy of California, Berkeley, 1956), Vol. III, p. 209.